Journal of the European Ceramic Society **19** (1999) 2405–2414
Published by Elsevier Science Limited
Printed in Great Britain
PII: S0955-2219(99)00129-6 0955-2219/99/$ - see front matter

Mechanical, Thermal, and Oxidation Properties of Refractory Hafnium and Zirconium Compounds

Mark M. Opeka,[a]* Inna G. Talmy,[a] Eric J. Wuchina,[a] James A. Zaykoski[a] and Samuel J. Causey[b]

[a]Naval Surface Warfare Center, Carderock Division, West Bethesda, MD, USA
[b]Southern Research Institute, Birmingham, AL, USA

Abstract

The thermal conductivity, thermal expansion, Youngs Modulus, flexural strength, and brittle–plastic deformation transition temperature were determined for HfB_2, $HfC_{0.98}$, $HfC_{0.67}$, and $HfN_{0.92}$ ceramics. The oxidation resistance of ceramics in the ZrB_2–ZrC–SiC system was characterized as a function of composition and processing technique. The thermal conductivity of HfB_2 exceeded that of the other materials by a factor of 5 at room temperature and by a factor of 2·5 at 820°C. The transition temperature of HfC exhibited a strong stoichiometry dependence, decreasing from 2200°C for $HfC_{0.98}$ to 1100°C for $HfC_{0.67}$ ceramics. The transition temperature of HfB_2 was 1100°C. The ZrB_2/ZrC/SiC ceramics were prepared from mixtures of Zr (or ZrC), SiB_4, and C using displacement reactions. The ceramics with ZrB_2 as a predominant phase had high oxidation resistance up to 1500°C compared to pure ZrB_2 and ZrC ceramics. The ceramics with ZrB_2/SiC molar ratio of 2 (25 vol% SiC), containing little or no ZrC, were the most oxidation resistant. Published by Elsevier Science Limited.

Keywords: borides, carbides, corrosion, mechanical properties, nitrides, thermal conductivity, thermal expansion.

1 Introduction

Hafnium and zirconium-based ceramics (carbides, borides, and nitrides) display a number of unique properties, including extremely high melting temperature and hardness, as well as high thermal and electrical conductivity and chemical stability. This combination of properties make these materials potential candidates for a variety of high-temperature structural applications, including engines, hypersonic vehicles, plasma arc electrodes, cutting tools, furnace elements, and high temperature shielding. The present investigation describes the thermal and mechanical behavior of HfB_2, HfC, and HfN ceramics synthesized by reactive hot pressing. Since HfC has a wide homogeneity range, variations in the properties as a function of carbon content were also investigated.

The ZrB_2-based ceramics were recognized early as relatively oxidation-resistant non-oxide refractory compounds. Research on these materials resulted in the development of ZrB_2/SiC ceramics which exhibited highly improved oxidation resistance over pure ZrB_2.[1] Recent investigations (NSWCCD, unpublished data) have shown that ZrB_2/ZrC/SiC compositions offer further improvement of oxidation resistance at very high temperatures (2200°C).

The present article describes the oxidation behavior of ZrB_2/ZrC/SiC ceramics at temperatures up to 1600°C as a function of component ratio. The ceramics were synthesized using *in-situ* high-temperature solid-state chemical (displacement) reactions. The advantage of the method is the possibility to create materials with novel and controlled microstructures, with high chemical compatibility of *in-situ*-formed individual phases, and phase distribution uniformity.

2 Experimental Procedure

The hafnium-based compounds were hot-pressed (75 mm diameter×15 mm thick billets) using −325 mesh powders from Cerac, Inc. (Table 1). Hafnium hydride (HfH_2) was added to all starting mixtures to decrease processing temperatures. The non-stoichiometric $HfC_{0.67}$ ceramics were prepared according to the reaction:

*To whom correspondence should be addressed. Fax: +1-301-227-4732; e-mail: opekamm@nswccd.navy.mil

$$67HfC + 33HfH_2 \rightarrow 100HfC_{0.67} + 33H_2$$

The ZrB_2/ZrC/SiC ceramics were synthesized from the starting mixtures consisting of Zr (Cerac, 99·7% purity, −325 mesh) or ZrC (Cerac, 99·5% purity, −325 mesh), SiB_4 (Cerac, 98·0% purity, −200 mesh), and C introduced as graphite (Cerac, 99·5% purity, −325 mesh). A series of samples in the system having progressively decreasing ZrC contents were synthesized in order to determine the effect of ZrC on the oxidation behavior of the materials. The ZrC/ZrB_2 molar ratios in the final ceramics were approximately 10:1, 4:1, 1:1, and 0:1, and the ZrB_2/SiC ratio was constant for all materials and equal 2:1. The synthesis and densification of ceramics were conducted during two-stage hot pressing: at 1750°C and 5 MPa for 1 h to complete chemical reactions and then at 2100°C and 20 MPa for 0·5 h for ceramic densification.

All materials were characterized by density (Archimedes method and helium pychnometry), phase composition (X-ray diffraction using a Siemens Theta-Theta Diffractometer), and microstructure (using a JEOL JSM-6400V Scanning Electron Microscope). For lattice parameter calculations in the HfC substoichiometric materials, an internal silicon standard was used.

Mechanical and thermal properties evaluated included elastic moduli, tensile strength, flexural strength, ductile-to-brittle transition temperature (DBTT), thermal conductivity, and thermal expansion (CTE). The test specimens were cut using electrical discharge machining (EDM) techniques.

The thermal conductivity of the materials was measured (sample size: 1·91 cm ∅×1·27 cm thick) using a comparative rod apparatus technique, which compares the conductivity of a specimen with the conductivity of a reference (iron and stainless steel for this effort). The thermal conductivity was calculated from the heat flow and temperature difference across a known gage length within the specimen at a given thermal input.

The CTE was measured (sample size: 0·64 cm ∅×5·08 cm long) up to 2500°C using two different dilatometers: a quartz-rod dilatometer provided data up to 1000°C and a graphite dilatometer up to 2500°C. The same specimens were used for both temperature ranges.

Table 1. The hot pressing parameters for processing billets

Material	*Temperature (°C)*	*Time (h)*	*Pressure (MPa)*
HfB_2	2160	3	27·3
$HfC_{0.67}$	2540	2	16·5
$HfC_{0.98}$	2500	0·67	31·7
$HfN_{0.92}$	2260	1	34·1

The tensile test of ring specimens (4·57 cm OD×4·06 cm ID×1·27 cm) utilized an internal, inflatable membrane to apply hydrostatic pressure. Top and bottom enclosure plates and annular retaining rings were used to ensure that the loading was applied in the radial direction.

Room and elevated temperature flexural tests were conducted (sample size: 0·30×0·635×4·318 cm) to determine strengths, moduli, and DBTTs. Flexural testing was conducted over a wide temperature range to determine the transition from elastic stress-strain behavior to elastic plus plastic deformation. The DBTT was determined from the change in slope of the load–deformation curve. The elastic moduli were determined from the measurement of ultrasonic velocity, as well as from ring tensile and 3-point flexural tests.

The oxidation behavior of the ZrB_2/ZrC/SiC ceramics was characterized by thermogravimetric analysis (TGA) using a TA Instruments SDT 2960 TGA/DTA module. The samples were heated at 20°C/min up to 1500°C in an argon/oxygen atmosphere, which simulated the concentration of O_2 in air. The TGA experiments were also conducted isothermally for 5 h at a series of temperatures. The oxidation behavior of the ternary ceramics was compared to that of pure ZrC and ZrB_2 ceramics prepared by hot pressing at 2300 and 2200°C, respectively.

3 Results and Discussion

X-ray diffraction (XRD) of the HfB_2 ceramics showed that it contained 5% HfC, likely due to the excess of hafnium metal being converted to the carbide during hot-pressing. The $HfN_{0.92}$, $HfC_{0.98}$ and $HfC_{0.67}$ ceramics were all determined to be single phase. The measured lattice parameters of $HfC_{0.98}$ and $HfC_{0.67}$ were 4·64331 and 4·62368 Å, respectively, correlating well with those reported in the literature.

All materials were well densified, as evidenced by SEM of polished sections, and density measurements. An open porosity of $< 1\%$ was measured for all samples, and total porosity was determined to be 5–10%. Figure 1 shows the microstructure of the materials. The HfB_2 ceramics [Fig. 1(a)] has a very fine-grained structure, with an average grain size of 10–20 μm, while the $HfN_{0.92}$ ceramics have a larger grain size of 40–60 μm. Both materials exhibit similar intergranular fracture pattern. The microstructure of the hafnium carbide ceramics showed a substantial dependence on carbon stoichiometry. The $HfC_{0.67}$ material [Fig. 1(c)] consisted of very large crystallites (> 200 μm in size), while $HfC_{0.98}$ [Fig. 1(d)] has a smaller grain size

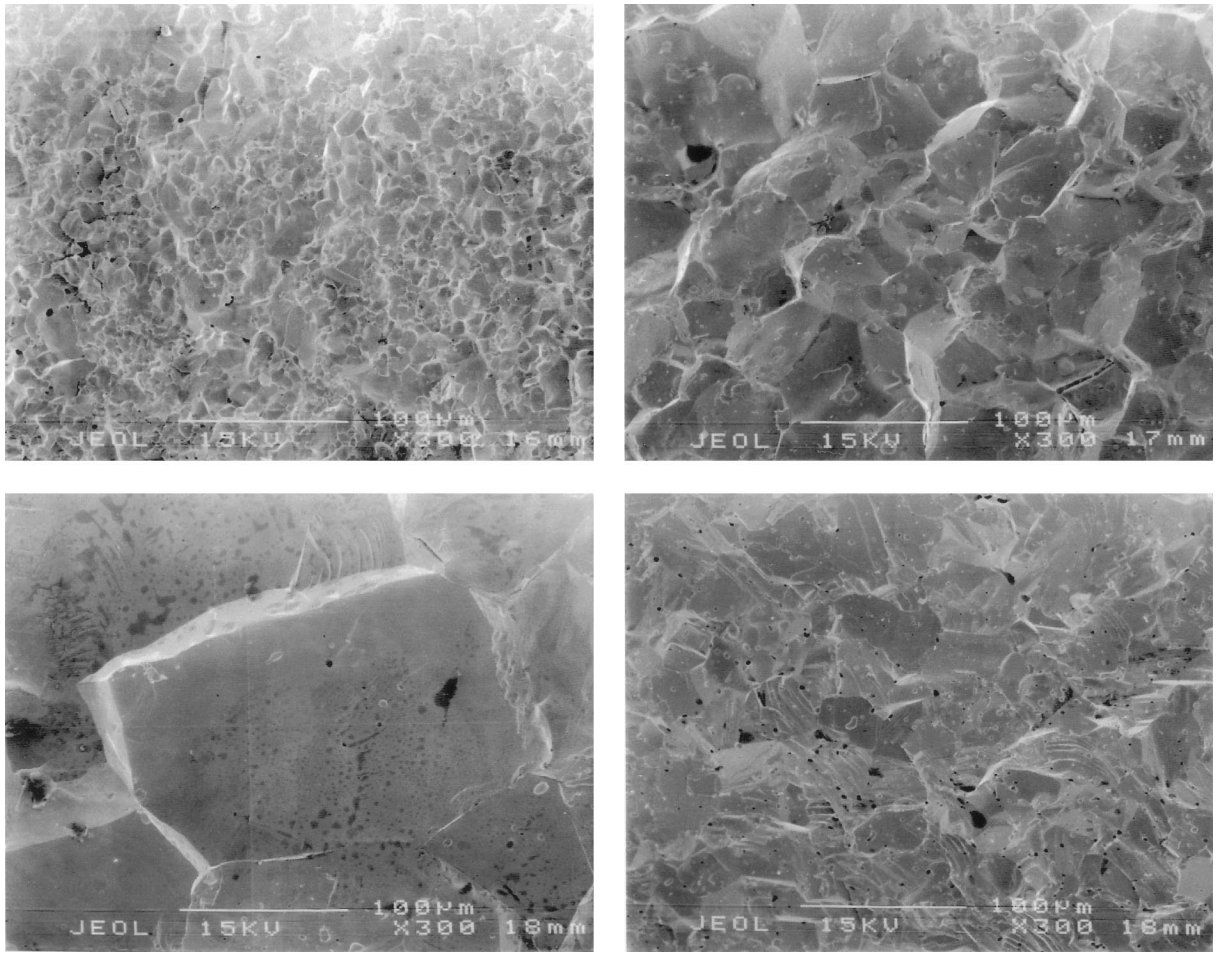

Fig 1. Scanning electron micrographs of (a) HfB_2, (b) $HfN_{0.92}$, (c) $HfC_{0.67}$, and (d) $HfC_{0.98}$.

(40–60 μm). The two carbide samples also exhibited distinctly different fracture behavior. The $HfC_{0.67}$ showed extensive intergranular fracture, while $HfC_{0.98}$ failed in an transgranular fracture mode, as evidenced by the flatter fracture surface.

3.1 Thermal and mechanical testing results

The thermal conductivities of the HfB_2, $HfC_{0.98}$, $HfC_{0.67}$, and $HfN_{0.92}$ ceramics are shown in Fig. 2. The conductivity of HfB_2 significantly exceeded that of the other materials: by a factor of 5 at room temperature and by a factor of 2·5 at 800°C. Additionally, the conductivity of HfB_2 decreased with temperature, while that of the other materials increased with temperature. Both carbides exhibited the same temperature coefficient of conductivity, but the conductivity of the $HfC_{0.98}$ exceeded that of the $HfC_{0.67}$ by a factor of two. This decrease in thermal conductivity can be due to increased phonon scattering from carbon vacancies in the substoichiometric carbide.

The thermal expansion curves of the all four materials were very similar in trend, as shown in Fig. 3. The expansion of all materials was approximately the same up to 1500°C. Above 1500°C, the $HfN_{0.92}$ ceramics exhibited some increase in the expansion rate.

Figure 4 shows the example of flexural stress-deflection curves for HfB_2 at 1090 and 1230°C. At 1090°C, almost purely elastic behavior up to specimen failure was observed. In contrast, at 1230°C, the deflection includes a significant plastic deformation component. Two modulus values were calculated from this curve based on the elastic and plastic components. All modulus data calculated from the flexural testing are shown in Fig. 5. For the $HfC_{0.98}$ sample, no plastic deformation was observed up to 2200°C. In contrast, the substoichiometric $HfC_{0.67}$ sample exhibited plastic deformation as low as 1090°C. This difference in behavior can be attributed both to the significant difference in microstructure (Fig. 1) and to the compositional difference (vacancy concentration) in two materials. The HfB_2 ceramics exhibited plastic deformation at a much lower temperature than the $HfC_{0.98}$ ceramics.

The room temperature Youngs moduli determined by all three techniques for $HfC_{0.98}$, and $HfN_{0.92}$ are shown in Fig. 6. The tensile testing-based data show very good agreement with the data gained from the ultrasonic velocity measurements. The modulus data calculated from the flexural testing are lower (by approximately 15%) for all four materials. The flexural test-based moduli

were expected to be low since the compliance of the load train is not accounted for in the calculation and utilized a short-span specimen. Of all four materials, HfB_2 exhibited the highest and the $HfC_{0.67}$ the lowest moduli.

3.2 Oxidation Testing Results

All ceramics in the ZrB_2/ZrC/SiC system were fully densified and had predicted component ratios. The microstructure of the ZrB_2/ZrC/SiC ceramics (Fig. 7) is very fine-grained with bigger (5–10 μm)

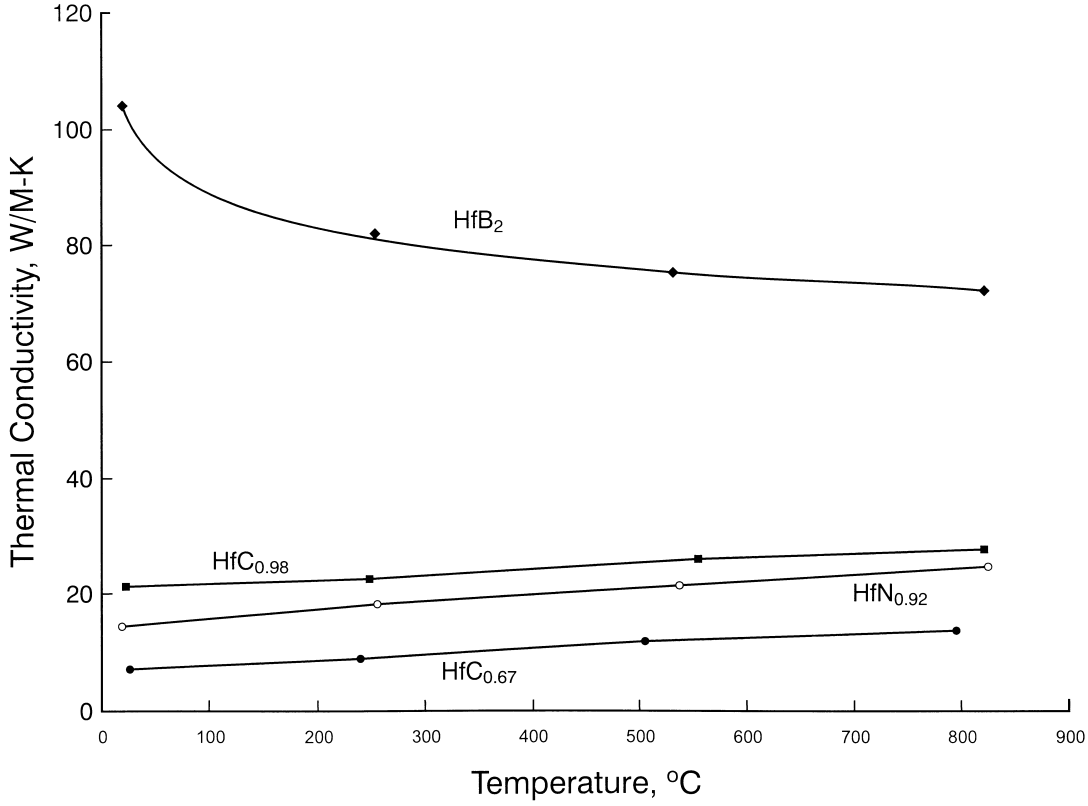

Fig. 2. The thermal conductivity of HfB_2, $HfN_{0.92}$, $HfC_{0.67}$, and $HfC_{0.98}$.

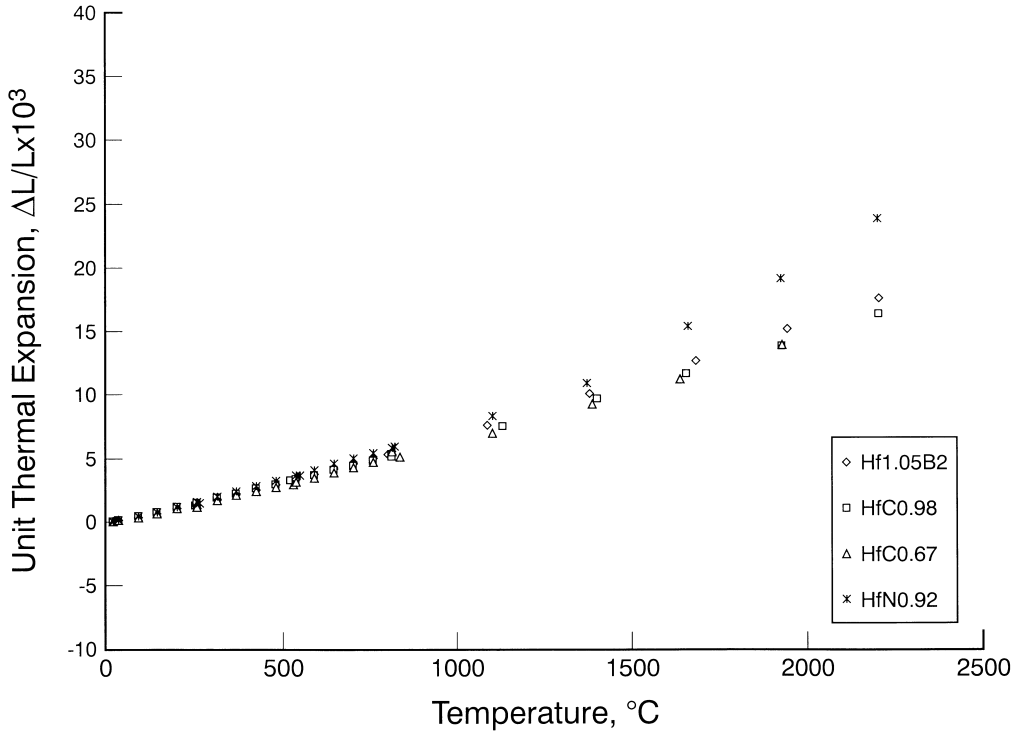

Fig. 3. The CTE of HfB_2, $HfN_{0.92}$, $HfC_{0.67}$, and $HfC_{0.98}$.

crystals of ZrB_2 surrounded by small submicron crystals of SiC and ZrC. Compared to that, the microstructure of the pure ZrB_2 ceramics is much courser with average crystal size of 30 μm. The presence of SiC and ZrC at the grain boundaries obviously inhibits excessive grain growth of ZrB_2 during processing.

The oxidation behavior of the ternary ceramics was compared to that of pure ZrC and ZrB_2. The pure ZrC (Fig. 8) was completely oxidized at 700°C during continuous TGA heating at 20°C/min. Comparatively, the ZrB_2 ceramics did not oxidize significantly even after 2 h heating at 1200°C (Fig. 9). The ceramics were protected by liquid boria

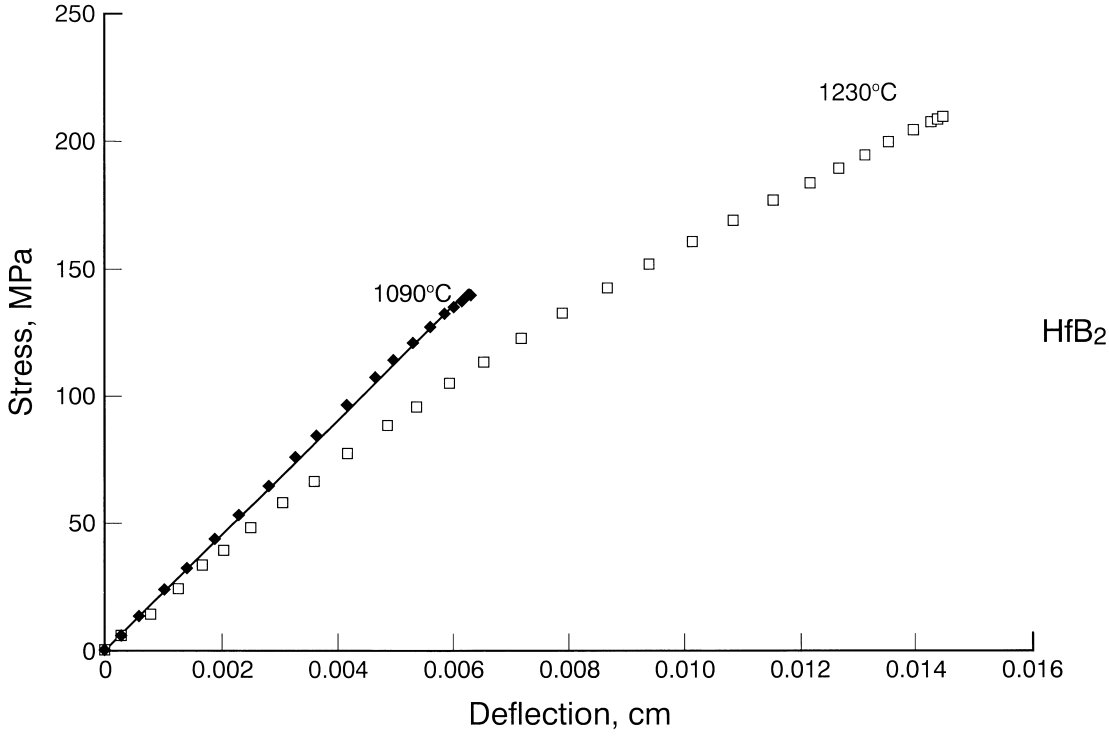

Fig. 4. The flexural stress versus deflection of HfB_2 at 1090 and 1230°C.

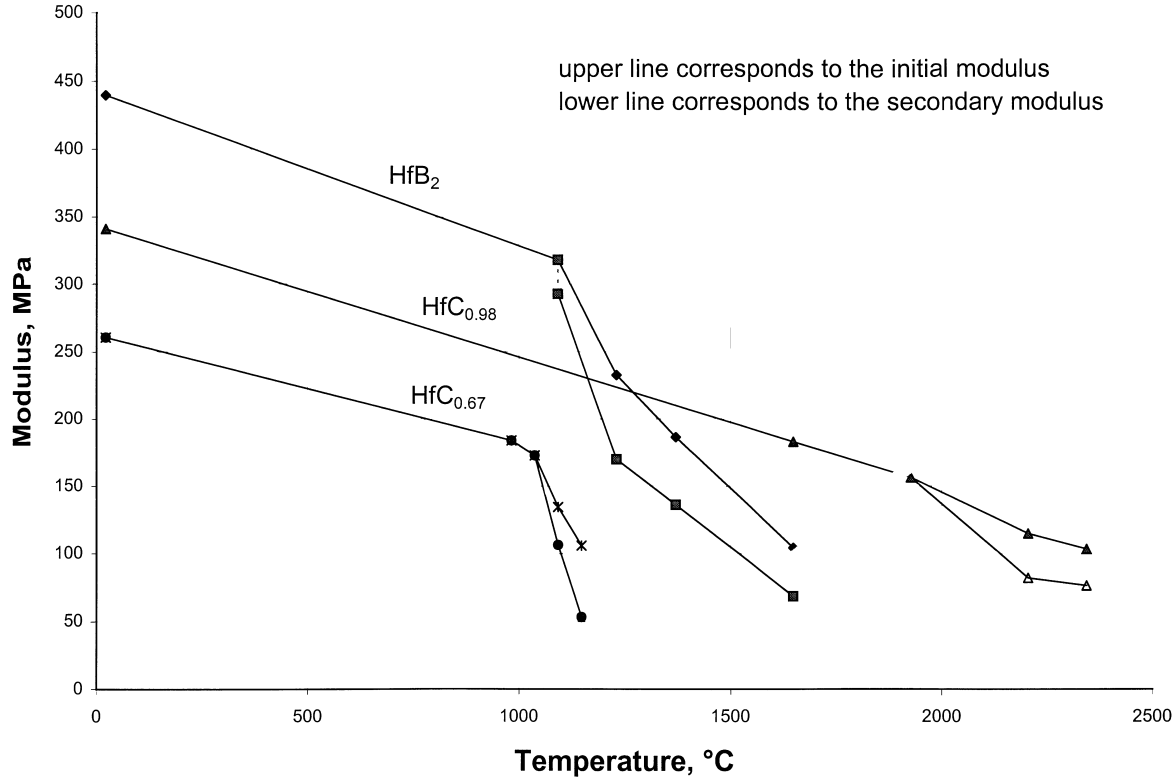

Fig. 5. Young's modulus versus temperature (from flexural testing) for HfB_2, $HfN_{0.92}$, $HfC_{0.67}$, and $HfC_{0.98}$.

observed by SEM (Fig. 10) directly below the surface between the ZrO_2 grains, which is indicated by the meniscuses between the ZrO_2 grains. Above 1200°C, pure ZrB_2 oxidized very actively due to the intensive evaporation of B_2O_3. However, calculations showed the presence of about 10 wt% (15 vol%) of boria even at 1400°C (Fig. 11), contradicting the literature data[2,3] claiming that, at tem-

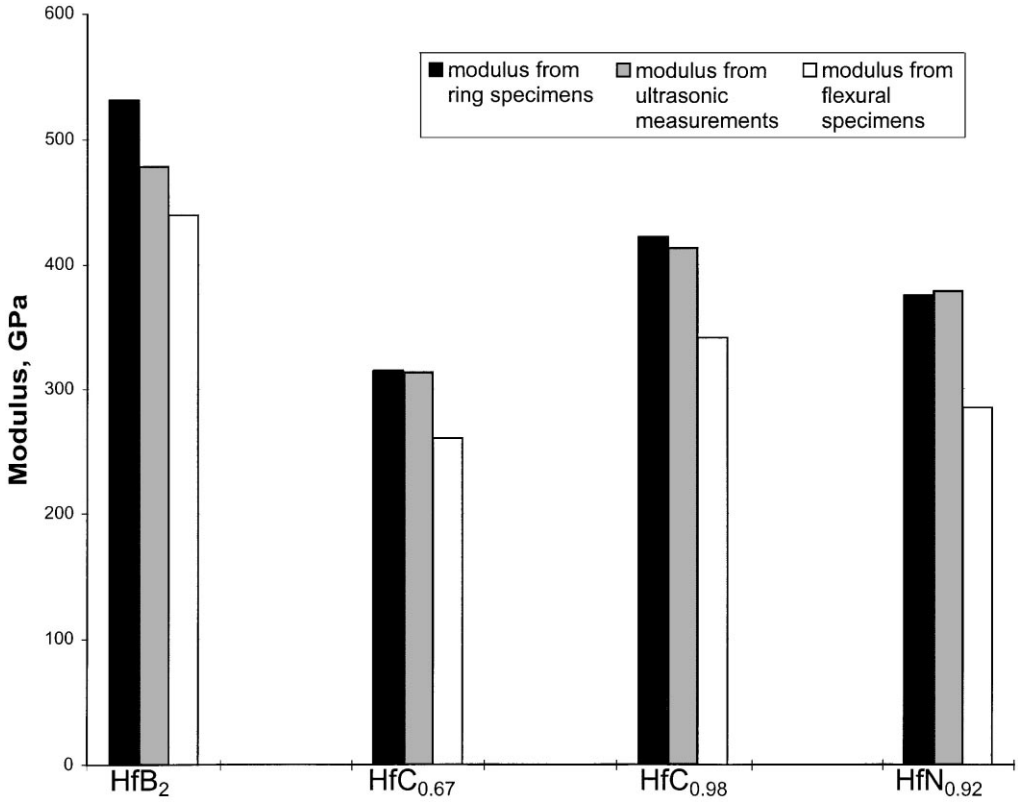

Fig. 6. The room temperature moduli of HfB_2, $HfN_{0.92}$, $HfC_{0.67}$, and $HfC_{0.98}$.

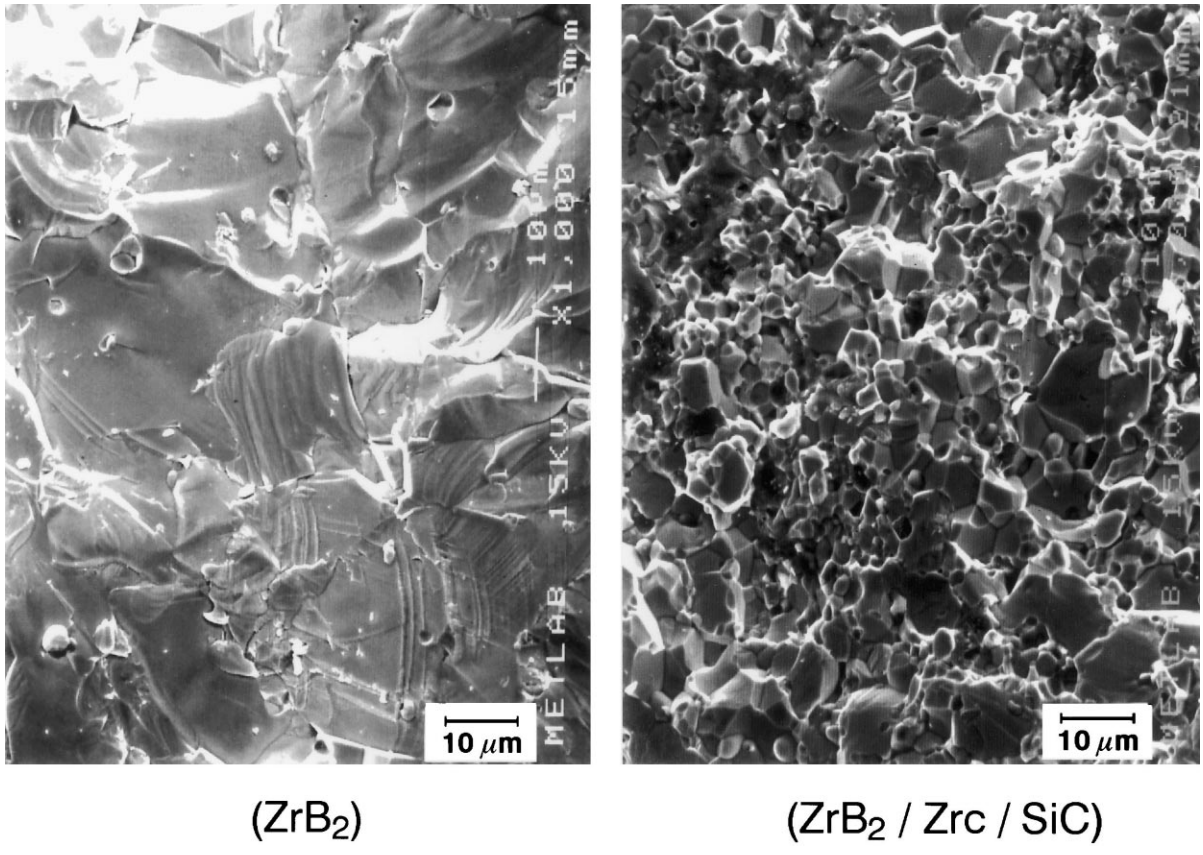

Fig. 7. SEM micrographs of ZrB_2 and ZrB_2/SiC/ZrC ceramics.

peratures above 1200°C, the vapor pressure of boria (m.p. 450°C and b.p.≈1850°C) becomes so significant that any boria formed during oxidation of ZrB_2 will completely evaporate.

The SiC-containing ZrB_2 ceramics (Figs. 8 and 9, curve with ZrC:ZrB_2 ratio of 0:1) showed low and thermally stable oxidation rate up to 1500°C. The thickness of the oxidized layer in this material stays at about 100 μm over the temperature range of 1200–1400°C after TGA heating for 5 hours (Fig. 12). For pure ZrB_2, the thickness of the oxidation layer increases as a function of temperature, confirming that boria alone does not prevent oxidation. The stability of both mass changes and thickness of oxidized layer with temperature for the ZrB_2/SiC ceramics is an indication of very low rate of oxidation which is due to the formation of a protective layer of borosilicate glass on the surface

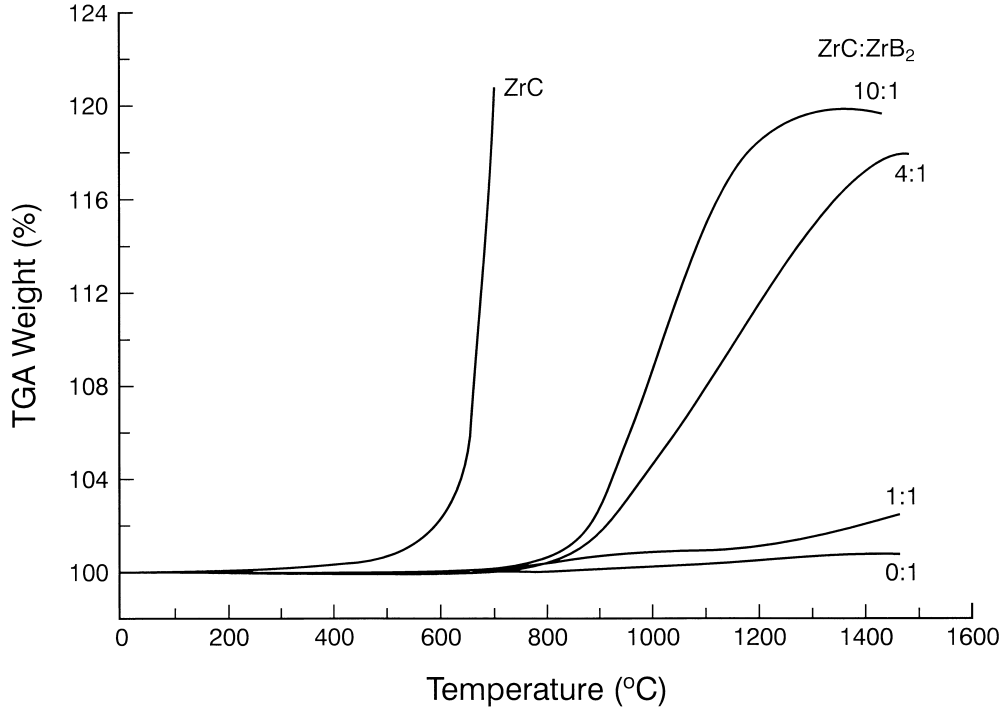

Fig. 8. Mass gain during TGA oxidation of ceramics in the ZrB_2/SiC/ZrC system as a function of ZrC/ZrB_2 ratio (ZrB_2/SiC ratio is equal 2).

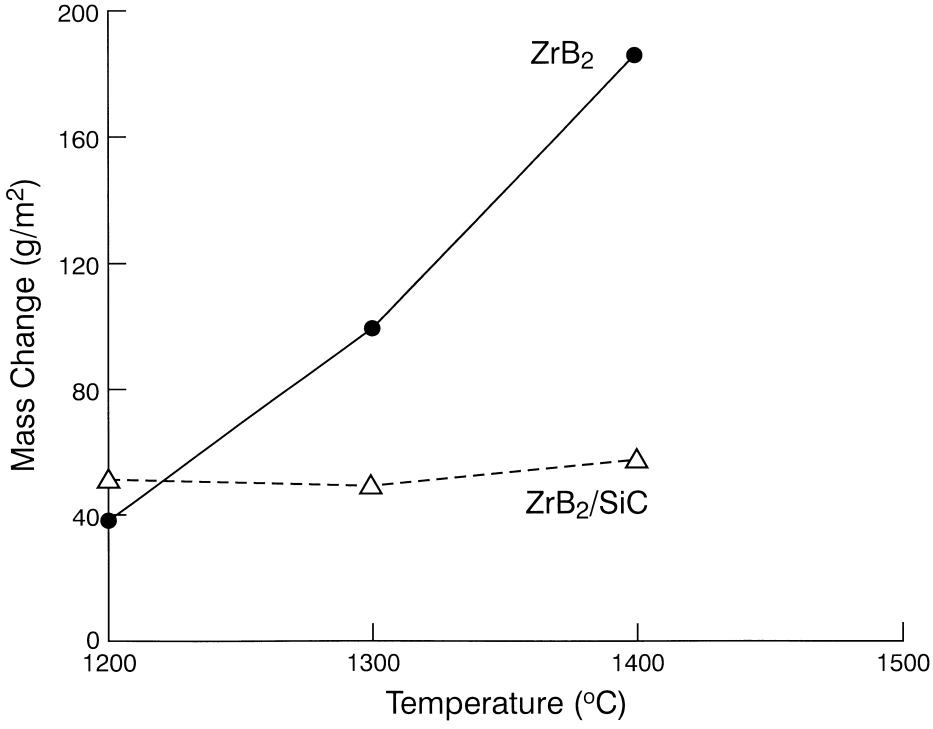

Fig. 9. Oxidation of ZrB_2 and ZrB_2/SiC ceramics in air (2 h).

of oxidized ceramics (Fig. 13). Compared to liquid B_2O_3 in ZrB_2, the borosilicate glass in the SiC-containing ZrB_2 ceramics has higher viscosity, higher melting temperature, lower oxygen diffusivity, and lower vapor pressure, thus providing much more effective oxidation-protective capabilities.

Practically similar oxidation rate of both ZrB_2 and ZrB_2/SiC ceramics below 1200°C is attributed to the formation of the surface scale consisting of ZrO_2 and liquid B_2O_3 since SiC does not oxidize appreciably at these temperatures to participate in the formation of borosilicate glass. However, at temperatures above 1200°C, the degree of SiC oxidation increases and becomes sufficient to form a protective layer of borosilicate glass.

The oxidation stability of the ZrB_2/SiC/ZrC materials (Fig. 8) increased with increasing ZrB_2 content. The low oxidation resistance of the ceramics having 10:1 and 4:1 ZrC:ZrB_2 molar ratios can probably be attributed to insufficient amounts of ZrB_2 and SiC to form a continuous protective surface layer of borosilicate glass during oxidation.

The analysis of the oxidation data for ZrC and ZrB_2 led to the development of a hypothesis describing the oxidation process. As it was mentioned, pure ZrC was completely oxidized at 700°C. The oxidation products are ZrO_2 and carbon oxides. The ZrO_2 forms a fine-grained porous scale which allows gaseous diffusion of O_2 through the pores to the ZrC surface, and therefore provides no oxidation protection.

In case of ZrB_2, the oxidation products are ZrO_2 and liquid B_2O_3. In the initial stage of oxidation, boria fills all of the porosity and grain boundaries

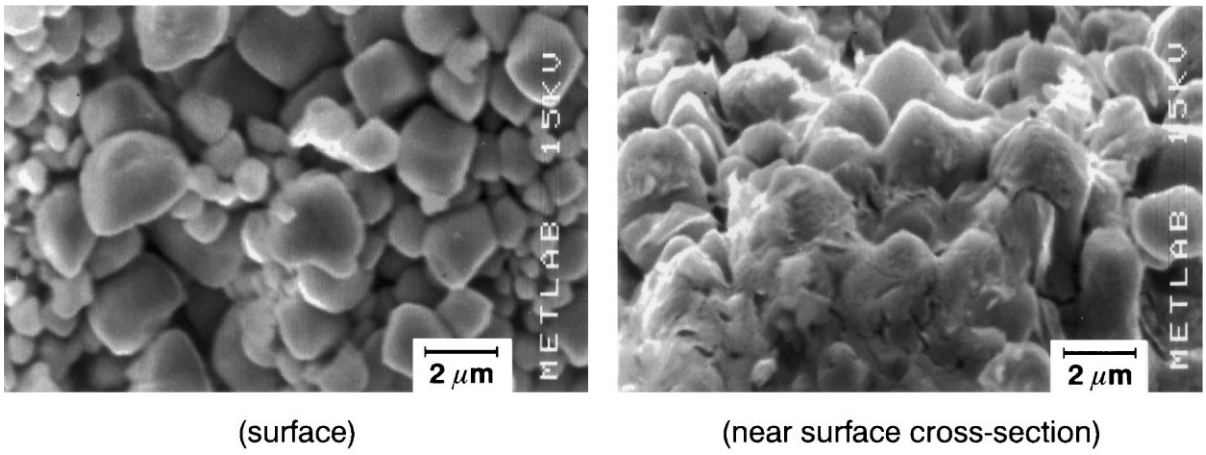

Fig. 10. SEM micrographs of ZrB_2 ceramics oxidized at 1300°C for 5 h.

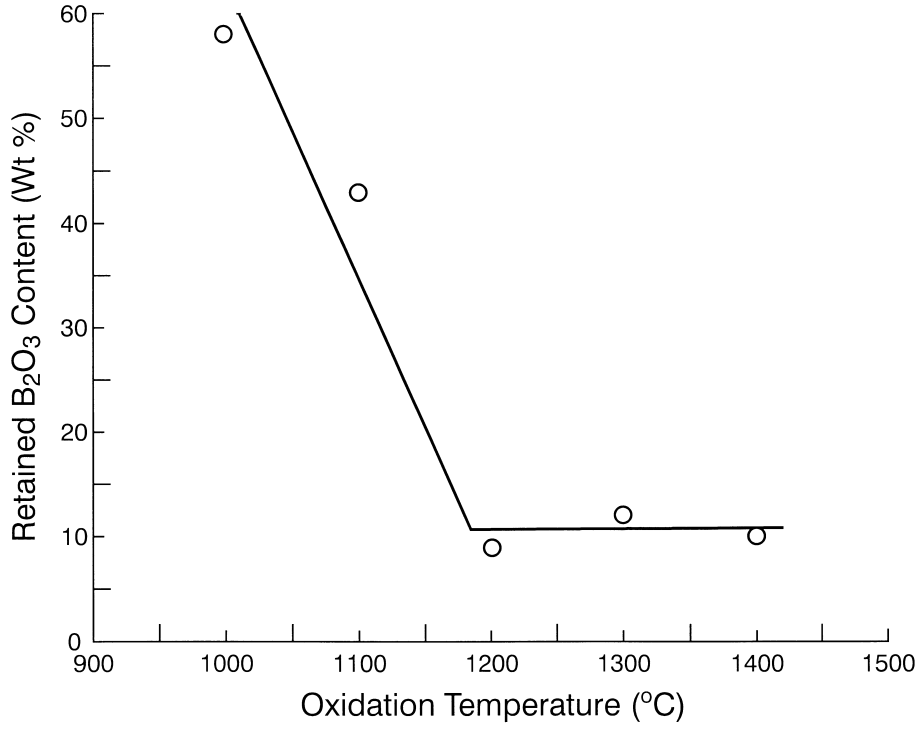

Fig. 11. Retained B_2O_3 content in the oxidation product of ZrB_2.

in the fine-grained zirconia forming continuous coating which prevents the gaseous diffusion of oxygen to the ZrB_2 surface and provides oxidation protection. As boria evaporates readily at temperatures above 1100°C, a condition arises in which only a thin layer of boria covers zirconia particles. Since the surface free energy of boria is only 0·08 J/m^2 compared to about 1 J/m^2 for zirconia, there is a large free energy driving force to keep the surface of zirconia covered with boria, providing an effective oxidation protection barrier even at higher temperatures.

The high surface free energy of the fine-grained zirconia explains the presence of boria in the oxi-

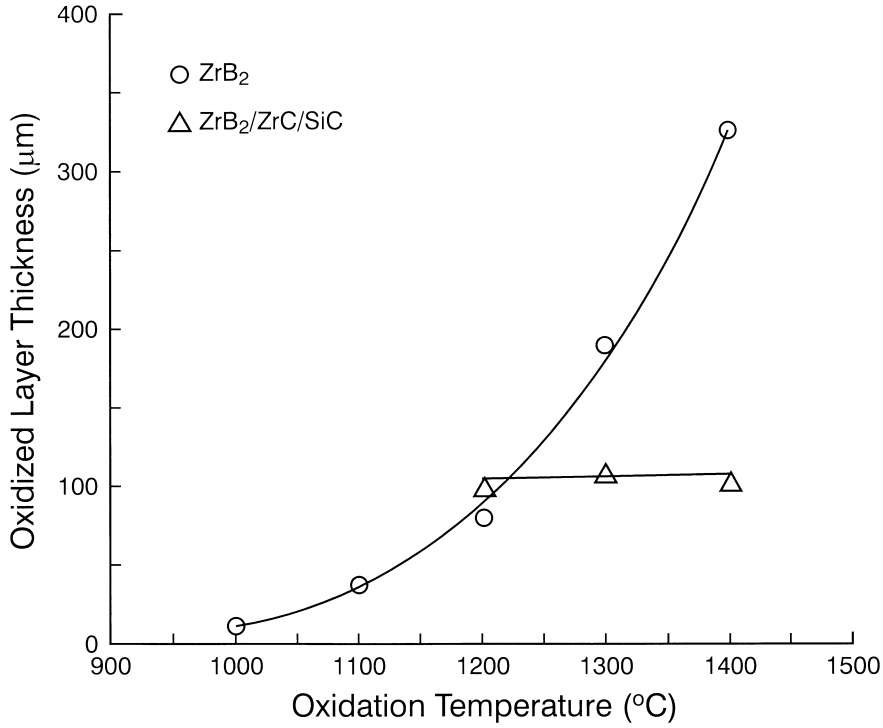

Fig. 12. Thickness of oxidized layer as a function of temperature after 5 h isothermal heating.

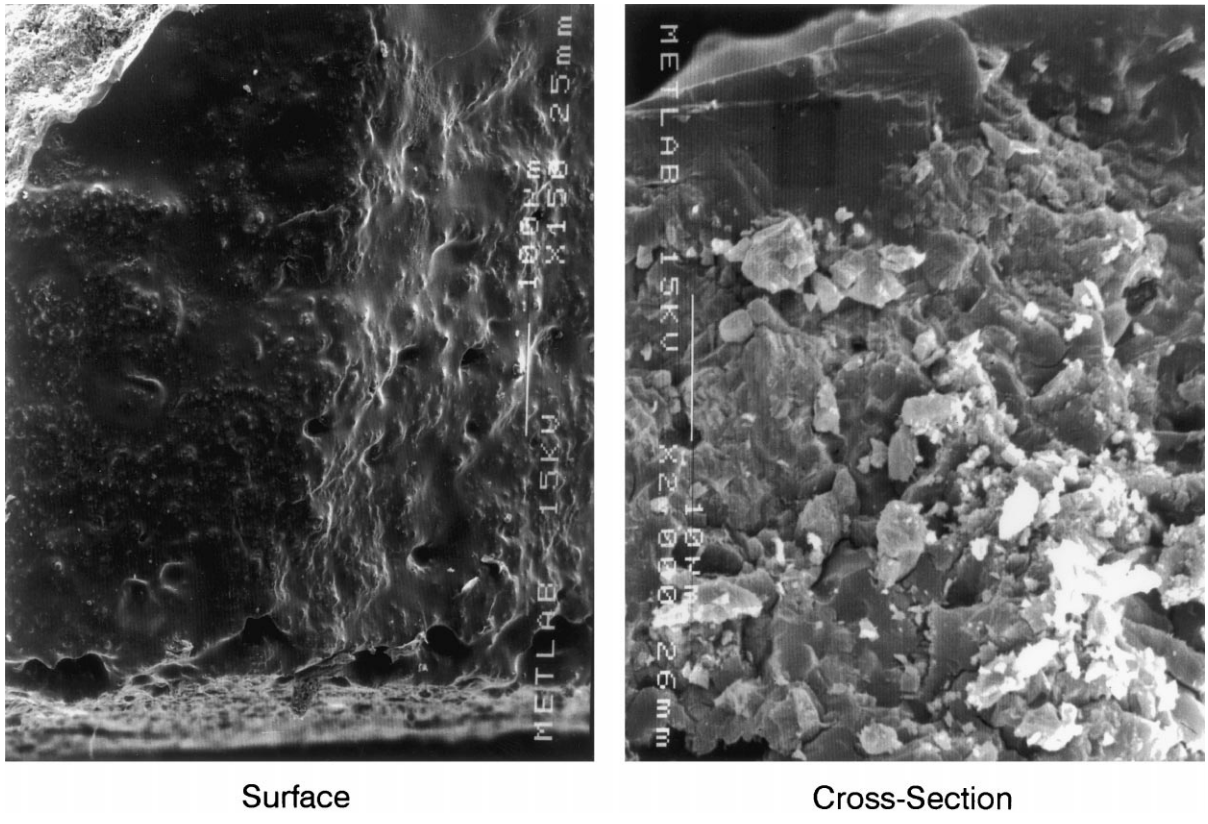

Fig. 13. SEM micrographs of ZrB_2/SiC oxidized at 1300°C for 5 h.

dized layer remaining constant at about 10 wt% (15 vol % of the oxidation products) at temperatures above 1200°C. However, regardless of the oxidation protection provided by liquid B_2O_3, the ZrB_2 oxidation process still occurs controlled by the diffusion of oxygen through the boria infiltrated zirconia layer. The formation of borosilicate glass in SiC-containing ZrB_2 provides much more effective oxidation-protective capabilities due to higher viscosity, higher melting temperature, lower oxygen diffusivity, and lower vapor pressure compared to B_2O_3.

4 Summary

The thermal and mechanical properties of hafnium-based nonoxide ceramics were measured. It was found that HfB_2 had a much lower ductile-to-brittle transition temperature than $HfN_{0.92}$ or $HfC_{0.98}$. The effect of lowering the carbon stoichiometry was also to decrease the transition temperature. The thermal conductivity of HfB_2 was much greater (by a factor of 5) than the carbides or nitride. The CTE of all materials tested were approximately the same up to 1500°C, with $HfN_{0.92}$ exhibiting a higher expansion than the others up to 2500°C. The HfB_2 ceramics had the highest modulus of the materials tested, while $HfC_{0.67}$ had the lowest. While the modulus measured during the flexural tests tended to be lower than those measured by the ring and ultrasonic methods, the trends between materials was consistent regardless of the measurement technique.

Ceramics in the ZrB_2/ZrC/SiC system were prepared from mixtures of Zr (or ZrC), SiB_4, and C using in-situ displacement reactions. The oxidation behavior of the ceramics was characterized as a function of phase composition which was varied by changing the of component ratios in the reactant mixtures. The SiC-containing ZrB_2 ceramics had high oxidation resistance up to 1500°C compared to pure ZrB_2 and ZrC ceramics. The ZrB_2/SiC ratio of about 2 (25 vol% SiC) is necessary for the best oxidation protection. The presence of ZrC in ZrB_2 ceramics negatively affects their oxidation resistance. A hypothesis describing oxidation behavior of the ZrB_2/ZrC/SiC ceramics is proposed.

Acknowledgements

The authors would like to thank Dr S. Dalleck and Mrs K. Witkoski of NSWCCD for conducting the TGA tests and assistance in SEM and EDS studies, respectively. The authors would also like to acknowledge N. Elsner and D. Allen of Hi-Z Technology, Inc. of San Diego, CA for the preparation of the hot-pressed billets. The NSWCCD Independent Research program and Dr S. Fishman of the Office of Naval Research provided support for this project.

References

1. Fenter, J. R., Refractory diborides as engineering materials. *SAMPE Quarterly*, 1971, **2**(3), 1–15.
2. Tripp, W. C. and Graham, H. C., Thermogravimetric study of the oxidation of zirconium diboride in the temperature range 800° to 1500°C. *J. Electrochem. Soc., Solid State Science*, 1971, **118**(7), 1195–1199.
3. Graham, H. C. et al., Microstructural features of oxide scales formed on zirconium diboride materials. In *Ceramics in Severe Environments*, Proceedings of the Sixth University Conference on Ceramic Science, North Carolina State University at Raleigh, 7–9 December 1970. Materials Science Research, Vol. 5. Plenum Press, New York, pp. 35–48.